Solar Energy Materials & Solar Cells 155 (2016) 88–100

Contents lists available at ScienceDirect

Solar Energy Materials & Solar Cells

journal homepage: www.elsevier.com/locate/solmat

Review

An insight into dislocation density reduction in multicrystalline silicon

Soobin Woo [a], Mariana Bertoni [b,c], Kwangmin Choi [a], Seungjin Nam [a], Sergio Castellanos [b], Douglas Michael Powell [b], Tonio Buonassisi [b], Hyunjoo Choi [a,b,*]

[a] *School of Advanced Materials Engineering, Kookmin University, 77 Jeongneung-ro, Seongbuk-gu Seoul, 136-702, Republic of Korea*
[b] *Department of Mechanical Engineering, Massachusetts Institute of Technology, Cambridge, MA 02139, USA*
[c] *School of Electrical Computer and Energy Engineering, Arizona State University, Phoenix, AZ 85004, USA*

A R T I C L E I N F O

Article history:
Received 27 January 2016
Received in revised form
29 March 2016
Accepted 31 March 2016

Keywords:
Multicrystalline silicon
Solar cells
Dislocation density
Pair-wise annihilation
Dislocation engineering

A B S T R A C T

Dislocations can severely limit the conversion efficiency of multicrystalline silicon (mc-Si) solar cells by reducing minority carrier lifetime. As cell performance becomes increasingly bulk lifetime–limited, the importance of dislocation engineering increases too. This study reviews the literature on mc-Si solar cells; it focuses on the (i) impact of dislocations on cell performance, (ii) dislocation diagnostic skills, and (iii) dislocation engineering techniques during and after crystal growth. The driving forces in dislocation density reduction are further discussed by examining the dependence of dislocation motion on temperature, intrinsic and applied stresses, and on other defects, such as vacancies and impurities.

Contents

1. Introduction

Despite the benefits of solar cells as a next-generation energy source, their high cost per wattage has kept them from achieving widespread use [1,2]. Although multicrystalline silicon (mc-Si) solar cells currently account for ~50% of worldwide photovoltaic

* Corresponding author at: School of Advanced Materials Engineering, Kookmin University, 77 Jeongneung-ro, Seongbuk-gu, Seoul 136-702, Republic of Korea.
E-mail address: Hyunjoo@kookmin.ac.kr (H. Choi).

http://dx.doi.org/10.1016/j.solmat.2016.03.040
0927-0248/

production owing to their low cost and scalability [3], conventional processes introduce many deleterious defects within the material, which deteriorate cell performance and hence offset the cheaper production costs [4,5]. For example, at a given cost target of electricity (~6 cents per kWh), an increase in the module efficiency from 10% to 20% allows an increase (from $10/m^2 to $75/m^2) in the module price [6].

Dislocations are well known as one of the most serious defects limiting the performance of mc-Si solar cells [7]. In principle, the reduction of dislocation densities from 10^6–10^8 cm^{-2} to as low as 10^3–10^4 cm^{-2} may lead to an improvement in the cell performance (from 13–14% to >20%). Hence, efforts have been made to suppress the harmful impact of dislocations on cell performance, to avoid the formation of dislocations during crystal growth [8,9] and to remove dislocations after ingot growth [10–13]. Despite numerous studies on the passivation of dislocations and the gettering of fast-diffusing metal impurities from dislocations, the improvement of cell performance after these processes is still very limited in regions with high dislocation densities (>10^6 cm^{-2}) [14]. One possible reason for this is that metal impurities and precipitates trapped in dislocation cores cannot be readily removed during gettering [15]. These impurities form deep-level recombination centers, which deteriorate cell performance [16]. Hence, alternative approaches for dislocation removal are required, in addition to gettering or passivation methods. Although technical reports on engineering dislocations during/after ingot growth have been published elsewhere; each work is concerned only with certain types of materials under certain conditions.

The present work departs from previous approaches in several respects. First, it reviews previous literature to provide a comprehensive understanding of (i) when dislocations are harmful, (ii) how they can be detected, and (iii) how they can be controlled in mc-Si. Second, it examines the underlying physics to clarify the thermal-mechanical conditions necessary to annihilate dislocations effectively. The effects of each key parameter, namely thermal input, activation energy for dislocation motion, and stress, on dislocation density reduction are investigated.

2. Impact of dislocations on the performance of Si solar cells

Extended crystal defects (e.g., dislocations, twins, stacking faults, and grain boundaries) interrupt crystal periodicity, inducing dangling bonds and deep states in the silicon band gap [17–20]. Stacking faults are relatively rare and twins are usually clean so they have negligible recombination activity in mc-Si [21,22]. Furthermore, Arafune et al. reported that the correlation between minority carrier lifetime and grain size is uncertain [17]. This is because the grain size of mc-Si is on the order of millimeters to centimeters, which is larger than the minority carrier diffusion length (generally less than 100 μm). Therefore, among crystal defects, dislocations are thought to be the most crucial defects limiting the photovoltaic performance of Si solar cells because they constitute the main source of recombination centers [23].

Dislocations act as recombination centers for electrons and holes by inducing deep trapping centers in the conduction and valence bands in Si. Dislocations primarily store carriers ejected from a band, and the extra carriers are promptly recombined when the source of excess carriers is removed. However, excess holes or electrons are ejected at a very low rate and the corresponding photocurrent decays very slowly, providing a slow and non-exponential recombination of holes and electrons, which deviates from the Shockley–Read theory. The space charge barrier surrounding the dislocation may have a dominant effect in determining the characteristics of recombination. Fig. 1 shows the

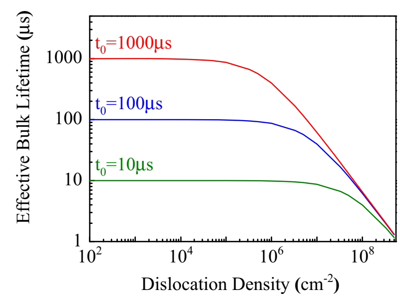

Fig. 1. Correlation between dislocation density and effective bulk lifetime, calculated using Donolato's model [7], for different dislocation-free lifetime (τ_0) of the Si bulk.

correlation between dislocation density and effective bulk lifetime, which is calculated using Donolato's model [7]. A significant degradation of the effective bulk lifetime of mc-Si is predicted as the dislocation density increases.

Although dislocations themselves may influence the electrical properties and photovoltaic performances of an mc-Si solar cell, significant additional degradation of the cell performance also occurs when dislocations are decorated with impurities. Dislocations are usually positively charged by holes in p-type silicon, and interact with carbon-related impurities (e.g., C_iO_i) or metal impurities so as to form a space charge region around the dislocations [24]. Block-cast mc-Si wafers exhibit areas of reduced lifetime around the wafer edges owing to impurities diffusing from the crucible wall into the silicon melt during solidification. At the boundaries, different grains meet and strain fields attract contamination, leading to an increased recombination activity [25]. Dissolved iron, iron complexes, and precipitates are known to introduce deep levels in the band gap, thereby increasing the carrier recombination rate. Precipitated iron has a less detrimental effect on lifetime compared to interstitial iron [26]. The higher concentration of Fe-B pairs is also the main cause for the deterioration of carrier lifetime in the order layer of the wafer [27]. Carbon and oxygen precipitation are also known as the decisive factor for a grain boundary acting as a current collecting defect [28].

The cell performance depends not only on the number of defects in the substrates, but also on how the defects are distributed [4]. On mc-Si wafers, the defect density is spatially inhomogeneous. Areas of high dislocation densities show very low short circuit current, and their influence on the total current is much more important than that of the grain boundaries. When dislocations are decorated with impurities, their influence on cell performance greatly varies according to their distribution [29]. Areas with high dislocation density introduce excess currents under reverse bias conditions, revealing hot spots through localized Joule heating of the material [30]. This significantly limits the photocurrent, the photovoltage, and the minority carrier diffusion length.

The geometric characteristics of the dislocation also affect the recombination behavior at the dislocations. In particular, recombination at dislocation loops [31] gives rise to dislocation-related radiation, which is attributed to local gettering, and thereby causing a large increase in the minority carrier lifetime. Furthermore, dislocation loops generate a local strain field, thereby providing efficient room temperature electroluminescence at the Si band-edge. It is more efficient when the loops are smaller and their density is higher because the individual strain fields are more readily overlapped with the closer dislocation loops [32]. The dislocation loop edge distorts the silicon lattice by applying a negative hydrostatic pressure to the adjacent silicon lattice just outside the loop. It was found that dislocation conduction may increase the dark current of solar cells [33]. However, dislocations in solar cells typically contain electrically disconnected segments, making it difficult to evaluate the conductivity of the dislocations. It is expected that in an ordered array of dislocations (i.e., dislocation networks) the conduction effect of dislocations is more significant.

3. Diagnosis of dislocations in Si solar cells

3.1. Direct observation of dislocations

3.1.1. Dislocation etching processes

One common way to observe defects in Si solar cells is the “defect etch”. Chemicals containing hydrofluoric acid (HF) repeatedly form and dissolve SiO_2 on Si. Eventually, etch pits are favorably formed at defect sites because the bonds around defects are weak and the electric charges around defects stimulate the etching process.

The so-called dash etch, which contains HNO_3, HF, and HAc (HAc is acetic acid [34]) reveals dislocations in all orientations, but it requires long etch times of 4–16 h. Afterward, several etching methods, such as the Sirtl etch (CrO_3 in water mixed with HF [35]), the Wright etch (CrO_3 and $Cu(NO_3)_2 \cdot 3H_2O$ in a mixture of water, HNO_3, HF, and HAc [36]), the Secco etch ($K_2Cr_2O_7$ in water mixed with HF [37]), and the Schimmel etch (a kind of modified Secco etch [38]), have been developed to employ oxidants as an alternative to HNO_3. The Sirtl and Wright etches form non-uniform etch pits according to the surface or grain orientations [37]. The Schimmel etch leaves a heavy stain on the samples. However, all these etchants contain metallic oxides, possibly contaminating the sample and clean processing area by leaving the remaining metallic ions. In response, Sopori developed an oxidant-free etchant (a mixture of HNO_3, HF, and HAc at a volume ratio of 2:36:15) [39].

Reimann et al. recently reported that dislocations are not revealed by the Secco etch when the Fermi energy level of the dislocations is unpinned in the highly doped p-type Si after long-term boron gettering. With a suitable etching solution for highly doped Si, the Wright etch in one case, dislocation etch pits are revealed even after long-term boron diffusion gettering [13]. On the other hand, when crystal defects are decorated with metals (e.g., Cu or Li), defect etching tends to be accelerated. Typical values for activation energies and selectivity of non-decorated dislocations are 29–33 kJ/mol and 1.95, respectively, while those of decorated dislocations are 25–34 kJ/mol and 3.0 [40].

Etch pits are generally observed using an optical microscope (OM) [41] and sometimes using a scanning electron microscope (SEM) [42]. A software package to quantitatively measure dislocation density, developed at MIT [43], is freely available online at http://pv.mit.edu/dlcounting/. Since the spatial resolution of defect etches is limited by etch-pit sizes (typically 3–6 μm), the measurable maximum dislocation density is below 10^7–10^8 cm^{-2}. Another limitation of this method is that it requires high-resolution microscope scanning with a spatial resolution better than 1 μm, which is time-consuming: 1-μm-resolution microscope scans takes ~1 h per square centimeter [44].

Commercial dislocation counting systems, such as PV scan [45], greatly accelerate image acquisition availability for statistical measurements on large-scale samples, but they are costly and are affected by errors if scanned areas contain other crystal defects (e.g., multiple twins) [46]. Needleman et al. recently developed a rapid dislocation counting method that can measure the dislocation density of 15.6×15.6 cm^2 wafers in less than five minutes using a flat-bed scanner [47].

3.1.2. Microscopic analyses

A number of microscopic analyses are available for defect observation in Si solar cells. Electron back-scattering diffraction (EBSD) is frequently used for simultaneous observation of defect morphology and crystallographic features [48]. An atomic-resolution transmission electron microscope (TEM) with high voltage provides high-resolution observation of dislocation activities at a theoretical resolution of up to ~1.9 Å [49]. For example, Kolar et al. have observed moving and stationary dislocation kinks and have measured the energies for kink formation, mobility, and unpinning based on TEM analysis [50]. Interaction between dislocations and other defects (e.g., Cu precipitation [51,52] and interstitial atoms [53]) is also addressed by TEM analysis. In situ TEM analysis enables researchers to observe real-time dislocation activities in Si under certain stresses and at high temperatures [54–56]. Ultra-high-vacuum reflection electron microscopy provides a new approach to revealing the micro-topography of their surfaces [57]. Annular dark-field scanning transmission electron microscopy (ADF-STEM) is less sensitive to the diffraction constant due to the convergent beam, thereby allowing large deviations from the exact Bragg condition to display dislocation images from the tilting series [58]. TEM analysis, combined with a secondary ion mass spectrometry (SIMS) technique, gives information about the interaction between point defects and pre-existing extended defects in silicon, through associated changes in the transient enhanced diffusion of boron [59]. Electron energy-loss spectroscopy (EELS) attached to TEM is useful for yielding valuable information about the electronic levels associated with dislocations using EELS spectra acquired on various dislocation cores in silicon [60]. Atom probe tomography (APT) is known to have a very high in-depth spatial resolution, enabled by an atom-by-atom field-evaporation process [61]. The accumulation of impurities on Si dislocation loops, the so-called Cottrell atmosphere, can be effectively detected using APT [62]. Neutron irradiation using optical and atomic force microscopes (AFM) gives information about the structure and deformation characteristics of Si [63].

Microscopy analysis with infrared, Raman, or X-rays is also useful for obtaining certain information about dislocation activities. Birefringence measurements, using a scanning infrared polariscope (SIRP) with high sensitivity, are useful for detecting residual stress induced by crystal detects throughout the sample [64]. Micro-Raman spectroscopy is a highly selective and sensitive technique for the probing of local atomic environments [65]. White-beam X-ray topography (WB-XRT) is widely used for the characterization of both long-range and short-range strain in single crystals [66–69]. High-resolution X-ray topography (XRT) provided quantitative measurements of misfit dislocation line density [70], together with the monitoring of in situ and real-time nucleation, growth, and movement of dislocations in silicon at high temperatures [71]. In situ XRT using synchrotron radiation during mechanical testing [72] or crystal growth [73] helped to reveal the mechanism of dislocation formation. A light beam–induced current map [74] also clarified the electrical effects of dislocations at different wavelengths, based on minority carrier diffusion length maps with deep-level transient spectroscopy. High-intensity synchrotron X-ray sources allowed in situ observation by XRT of a low density of dislocation segments moving in silicon samples of a whole gauge length of during creep experiments [75]. A technique using symmetric reflection via an azimuthal rotation of a sample was employed to characterize the three-dimensional distribution of dislocations in single crystals. An analytic formula was derived to transform the three-dimensional geometry of a straight dislocation into its two-dimensional projection onto the detector plane. By fitting topography to the formula, the orientations and locations of dislocations were quantitatively determined [76]. A combination of a

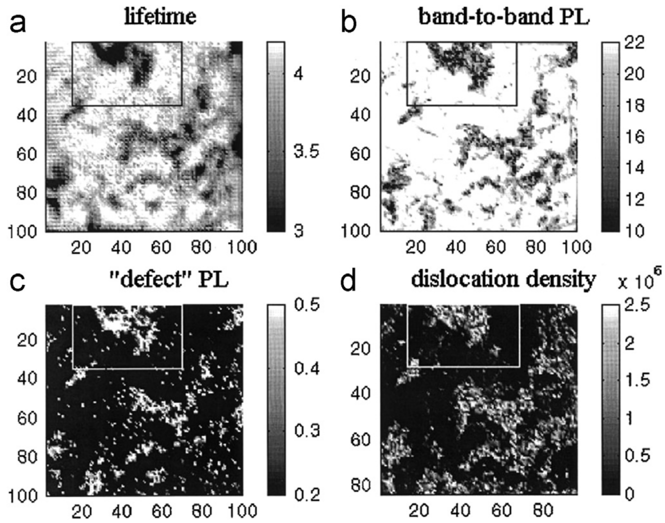

Fig. 2. (a) Minority carrier lifetime mapping with laser-microwave reflection; (b) band-to-band PL intensity (290 K); (c) 'defect' PL intensity (290 K); (d) dislocation density measured by EPD technique [79].

number of microscopic techniques provides substantial information about dislocation activities in Si. For example, a combined technique of X-ray and Fourier transform infrared spectroscopy (FTIR) mapping [77] clarified the mechanism for the generation of structural defects in directionally solidified mono-like Si.

3.2. Indirect diagnosis of dislocations

The effect of the presence of dislocations on the electrical behavior of Si solar cells can be diagnosed using a variety of techniques that use electrons or photons. Owing to their high spatial resolution, electron-beam induced-current (EBIC) and light-beam induced-current (LBIC) are considered to be the most suitable techniques for studying the recombination characteristics of an individual extended defect in a semiconductor [78]. These techniques are effective for detecting the segregation behavior of metallic impurities on individual extended defects. As shown in Fig. 2, photoluminescence (PL) spectroscopy, combined with laser-microwave reflection and dislocation etch mapping, can be applied to obtain a spatially resolved defect diagnosis in mc-Si ingots and to assess the corresponding electronic properties of high-quality solar-grade materials [79].

Deep-level transient spectroscopy (DLTS) was used to identify electrically active defects and the interaction between impurities and dislocations [80,81]. Dislocation networks formed by silicon wafer bonding were analyzed using a combination of EBIC and PL analyses [33]. DLTS is also facilitated by combining EBIC or LBIC techniques to address dislocation-impurity interaction [82] and to detect electrically active defects [83]. The LBIC mapping technique at different wavelengths together with DLTS enabled researchers to recognize and detect these arrays and to evaluate their recombination strength [84]. A comparison of various techniques may provide precise information about dislocation behaviors [85]. The use of direct-current, continuous–operation, glow discharge mass spectrometry (GDMS) has become an established technique for multi-element investigation of trace- and ultra-trace impurities in highly pure metals and semiconductors [86].

PL mapping or microwave-detected photoconductivity (MDP) have been frequently employed for in-line low-quality diagnosis of. PL imaging has been introduced as a fast tool for imaging the lifetime of a wafer, i.e., its diffusion length or iron contamination. Using PL imaging, the lifetime can be acquired with high spatial resolution. The generation of dislocations during crystal growth and areas of reduced lifetime were detected at the edges of the crystallization crucible and near the top or bottom of a brick in the line [25]. MDP and surface photovoltage measurement are established techniques for the measurement of FeB concentration. The FeB concentration was determined from the lifetime before and after optical dissociation of iron–boron pairs [87–89]. It was recently confirmed that an SIRP is also useful in monitoring the device processes of silicon wafers [90].

These measurements can also be compared with microscopy analyses. EBIC analysis with a defect etch, micro-Raman spectroscopy, and EBSD analysis have been used to clarify the influence of defects in stress fields on the electrical activity and residual stress states of as-grown edge-defined film-feed mc-Si ribbons. EBIC was used to evaluate the recombination activity of dislocations, while defect etching, micro-Raman spectroscopy, and EBSD were used for visualization of surface defects, millimeter-scaled internal stress fields, and the features of crystalline orientations and crystalline boundaries, respectively [91]. A new electron diffraction technique for obtaining direct experimental evidence of dislocation core structures was developed by combining electron spin resonance, the Hall effect, deep-level transient spectroscopy, etch-pit measurements, X-ray topography, internal friction measurements, and in situ TEM [92]. Highly spatially resolved PL and EBSD techniques were used to observe the characterization of harmful defects (by PL) and the effect of the grain angle, grain orientation, and other grain parameters (by EBSD) [93]. It also provided information about the three-dimensional structure of the intragrain defects [94]. A combination of grain boundaries and point defects with high recombination activity was detected by X-ray fluorescence, EBIC, EBSD, and a defect etch [17]. PL or cathodoluminescence (CL) imaging combined with a defect etch, SEM, or TEM was used to address the formation [95] or annihilation mechanisms [96] of dislocations together with recombination activities in dislocations [26].

4. Dislocation engineering in Si solar cells

During the processing of Si solar cells, two main techniques are used to reduce the impact of defects and improve the performance of mc-Si materials: (i) passivation of crystal defects with atomic hydrogen that diffuses from a SiN_x: H coating layer into bulk silicon during contact co-firing and (ii) gettering of fast-diffusing metal impurities during phosphorus diffusion and aluminum back contact formation, which is based on the enhanced metal solubility in the p-diffused layer and the liquid Al-Si layer. Grain boundaries and dislocations in mc-Si are sinks for doping impurities and contamination, including oxygen [79,94]. However, it was observed that hydrogen passivation may be insufficient to eliminate the detrimental effect on carrier lifetime of oxygen precipitates at grain boundaries and dislocations [74]. Phosphorus gettering has been found to effectively remove the interstitial iron atoms and fully recover the lifetime of minority carriers in a low dislocation density region in Si [97]. However, a high dislocation density affects the effectiveness of gettering in removing metallic impurities. It suppresses the gettering effect, resulting in reduced conversion efficiency [98]. Therefore, a great deal of effort has been made to develop techniques for suppressing the generation of dislocations during crystal growth or for annihilating dislocations via post-annealing.

4.1. Suppression of dislocation generation during crystal growth

Dislocations are mainly generated during crystal growth as a result of thermal stresses and different crystal orientations. A model was developed based on the constitutive Alexander–Haasen–Sumino model to describe the nucleation of dislocation clusters during crystal growth near the solid–liquid interface [99]. Anisotropy in the elastic modulus of Si, stemming from the different crystal orientations, introduces shear stress to the slip plane and generates dislocations. The dislocation density was also found to rapidly increase during the cooling process after solidification of the ingot [100]. During directional solidification, Si crystals are subjected to compressive forces from a crucible because the Si crystals expand by approximately 10% in volume when the Si melt is crystallized. Lambropoulos and Wu conducted a numerical analysis to calculate the effect of cooling rate on dislocation density in a Si ingot [9]. The maximum dislocation density in the silicon ingot using a cooling rate of 1.2 kW/h was about 1.5 times larger than that using a cooling rate of 4.7 kW/h, even though the maximum value of the residual stress in the Si ingot using a cooling rate of 4.7 kW/h was about three times larger than that using a cooling rate of 1.2 kW/h. Interestingly, the results showed that a fast cooling process, with large residual stress, introduces a low dislocation density, which contradicts the experimental observations reported elsewhere [101].

PL imaging combined with microscopy analysis was used to detect intragrain defects in mc-Si. Several important findings have thus far been reported: (i) the dislocations occur at the grain boundaries (GB), (ii) dislocations propagate as growth proceeds, (iii) dislocations are introduced near the solid–liquid interface during directional solidification and the initially generated dislocations act as the source of other dislocations, (iv) dislocations occur only in one grain at the GB, and (v) a rapidly solidified wafer has a higher defect density than a slowly solidified one. Hence, dislocation size and density depend on crystallographic orientation and growth conditions [94]. Furthermore, as the temperature of the Si ingot decreases, the rate of generation of dislocations also gradually decreases. The microstructure evolution, solid–liquid interface, and dislocation structure under different growth conditions revealed that (i) the distribution of dislocations is highly inhomogeneous among the grains and (ii) the dislocations are arrayed in the form of dislocation clusters, showing a typical slip dislocation characteristic [102]. They also indicated that the generation of crystal defects, such as dislocations or twin boundaries, is highly related to the characteristics of grain boundaries. The role of the grain boundaries is shown in Fig. 3 [103]. Fig. 3(a) shows that most dislocation seed clusters were generated in the lower part of an ingot and Fig. 3 (b) clearly reveals that most (~91.7%) dislocation cluster seeds have their origin at grain boundaries. While ~5.6% of cluster seeds are formed at triple junctions, over 97% of all cluster seeds have a connection to a grain boundary [13,103].

Some researchers have attempted to reduce dislocation density during Si ingot growth by adjusting process parameters [10–12]. The square root of the maximum dislocation density was found to correspond to the difference in the cooling flux in radial or axial directions, which denotes that the energy accumulation and dissipation rates inside the whole crystal are respectively controlled by the expansion and contraction rates of the crystal, thereby determining the applied stress levels [104]. A slightly concave interface may lead to dislocation-free growth, while a highly concave interface could introduce dislocations through plastic deformation. Several groups have tried to utilize dendritic growth [105–107] in the initial stage of crystal growth to achieve mc-Si with controlled crystalline orientation and large grain size. They proposed a seeded-growth technique to grow mc-Si with a monocrystalline-like (mono-like) structure, which has fewer defects than conventional mc-Si ingots. Thermal-stress-induced dislocations can also be suppressed through the doping effect. Doping with electrically active impurities in Si controls the Fermi energy level of dislocations and induces supersaturation of vacancy-like defects, thereby suppressing dislocation formation.

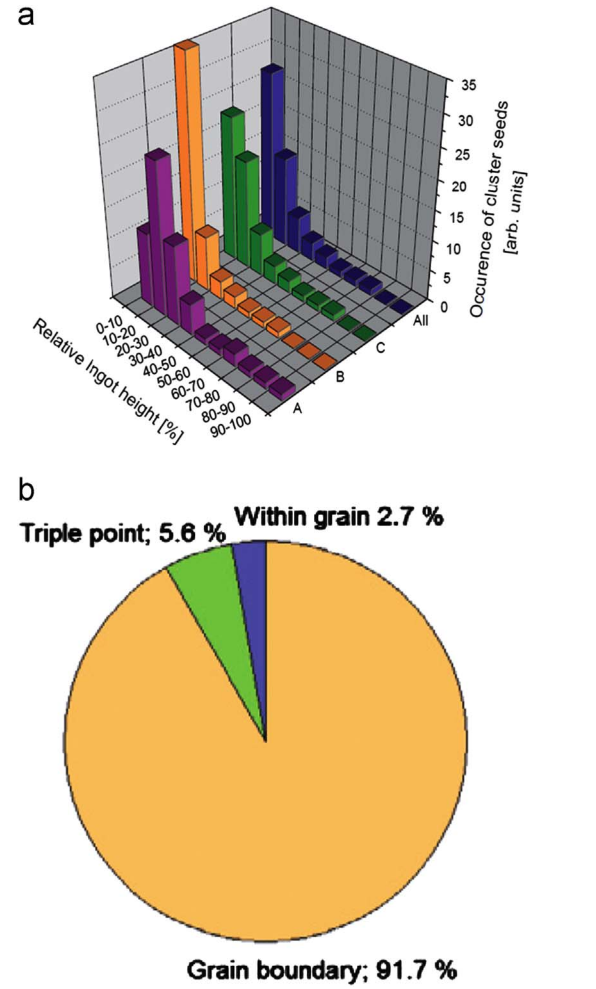

Fig. 3. (a) Occurrence of dislocation cluster seeds over ingot height. Blue (All): all investigated bricks. Magenta (A), orange (B), and green (C): groups of growth processes showing different behaviors in cluster seed generation; (b) diagram showing the relative frequency where cluster seeds occur regarding to grain structure [103]. (For interpretation of the references to color in this figure legend, the reader is referred to the web version of this article.)

4.2. Reduction of dislocation density after crystal growth

4.2.1. Physics of dislocation activities

A considerable number of investigations have been conducted on the modeling and simulation of the dynamic behavior of dislocations [108–111]. Furthermore, several attempts have been made to quantitatively examine the effect of stress and temperature on dislocation mobility in mc-Si in experiments [108,112,113]. The results indicated that dislocation mobility increases with temperature and stress, which is consistent with the Peierls–Nabarro model [112]. However, some research, such as large-scale atomistic simulations on a 60° dislocation motion in Si for temperatures ranging from 100 to 900 K and applied stresses ranging from 100 to 3000 MPa [112], revealed that dislocation velocity decreases as the temperature increases. According to the phonon drag model [108,113], thermal phonons inherent in a crystal lattice scatter from a moving dislocation and thereby dampen the dislocation motion. This phonon damping effect is proportional to the temperature.

A technology flow chart describing the underlying physics and practical techniques for dislocation density reduction is shown in Fig. 4. The prevailing hypothesis for dislocation density reduction is that annealing in the presence of a driving force (e.g., high thermal fluctuations and mechanical stresses) results in pairwise dislocation annihilation (dislocations with the opposite sign attract each other

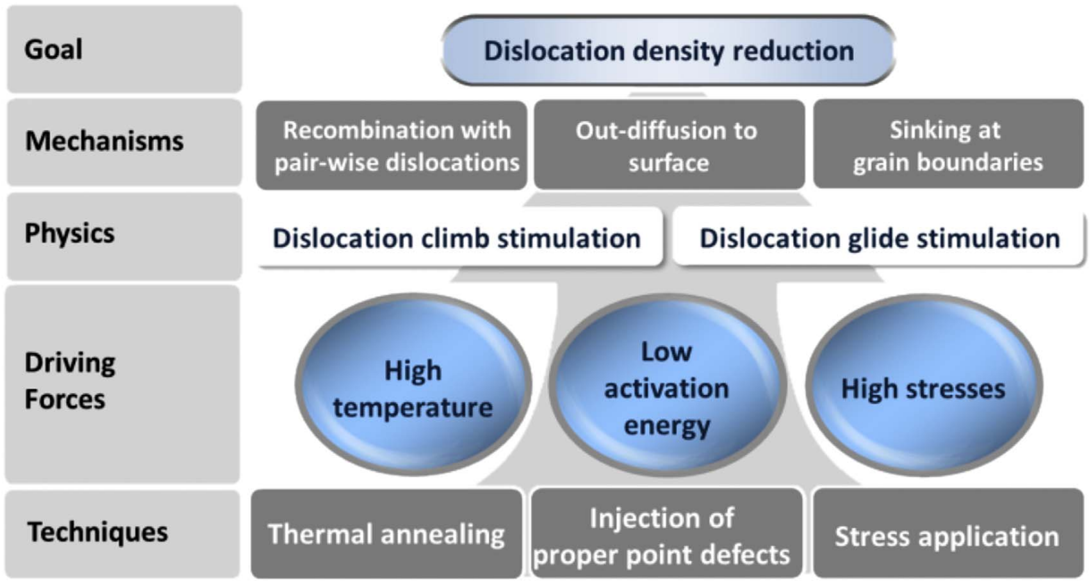

Fig. 4. A technology flow chart for dislocation density reduction.

Table 1
Studies of relationships between annealing temperature and dislocation density reduction behavior.

Authors	Materials	Annealing profile	Results
Hartman et al. [115]	Ribbon MC-Si	Annealing temperature: 1100, 1233, 1366 °C Annealing time: 6 h Heating rate: 20 °C/min Cooling rate: 7 °C/min	Dislocation density reduction according to the models of Kulmann and Nes
Xu. et al. [120]	UMG-Si ingot	Annealing temperature: 1160, 1260, 1360 °C Annealing time: 6 h N_2 atmosphere	Dislocation density reduction but reduction of minority carrier lifetime and resistivity of the wafers as the annealing temperature increases
Wu et al. [121]	UMG-Si ingot	Annealing temperature: 1000, 1100, 1200, 1300 °C Annealing time: 3 h Heating rate: 10 °C/min Cooling rate: 10 °C/min pure Ar atmosphere	(1) The arrange order of dislocation density of UMG-Si ingot from the lowest in the bottom and low in the top before and after annealing (2) Dislocation density reduction with an increase of annealing temperature
Stokkan et al. [122]	MC Si ingot	Annealing temperature: 1350 °C Annealing time: 4 h Heating rate: 20 and 7 °C/min Cooling rate: 7 °C/min	Dislocation density reduction near the sample surface.(area within 50 μm from the surface)

and annihilate pairwise) or out-diffusion of dislocations to surfaces at high temperatures. Dislocations become mobile within certain crystallographic glide planes at temperatures above the brittle-to-ductile transition temperature (i.e., 530–660 °C for Si, depending on dopant concentration and strain rate) [114]. Vacancy diffusion causes dislocations to climb out of the glide plane at temperatures above 1000 °C. Driving forces, such as thermal fluctuations and mechanical stresses, are required for dislocations to overcome a certain amount of activation energy to be mobile. Hence, higher temperatures, lower activation energy, and a sufficient amount of stress may lead to an enhancement of the dislocation velocity or the rate of reduction of dislocation density.

Within this scope, a number of technologies to reduce dislocation density in mc-Si have thus far been suggested. A high-temperature isothermal annealing near the melting point has been reported to result in significant reduction in dislocation density [115,116]. It has been proposed that small amounts of external stress [116] or the presence of a unidirectional flux of point defects [117] may stimulate dislocation motion, accelerating the annihilation of dislocations.

4.2.2. Effect of temperature

Table 1 summarizes the research on the relationship between temperature and dislocation density reduction. Although the experimental details, such as the starting materials, annealing atmosphere, and cooling profile, are varied, they exhibit similar tendencies. Hartman et al. reported a significant dislocation density reduction (>95%) after high-temperature (i.e., 1366 °C) annealing, following the models of Kuhlmann [118] and Nes [119]. Xu et al. [120] also reported that dislocation density can be reduced after thermal annealing, while the minority carrier lifetime decreases as annealing proceeds. Dislocation density was found to vary according to location in an ingot; it was lowest in the middle and highest in the top, both before and after thermal annealing [121]. A number of metal impurities may impede dislocation annihilation processes in the top of the ingot. Stokkan et al. [122] reported that annealing of mc-Si at 1350 °C for 4 h

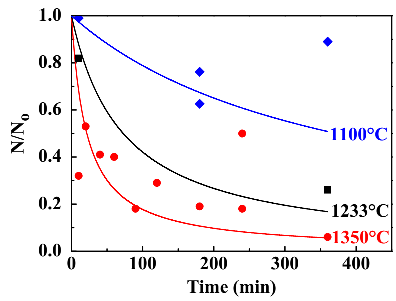

Fig. 5. Dislocation density reduction as a function of annealing time and temperature (data obtained from studies in Table 1).

results in a dislocation density reduction within 50 μm from the sample surface.

In general, the dislocation density decreases with the increasing annealing temperature and time. Experimental data from the studies in Table 1 are plotted in Fig. 5. The data is also compared with the theoretical calculation according to the models of Kuhlmann [118] and Nes [119]:

$$\frac{dN}{dt} = -K \cdot exp - \frac{Q - \beta GN/L}{k_B T},$$

where N is the dislocation density after annealing, t is the time, K and β are constants, Q is the activation energy, L is the length of each slip line, k_B is the Boltzmann constant, and T is the temperature. According to the theoretical calculation, the dislocation density reduction increases with the increasing annealing temperature and time. Since the experimental data were obtained from different materials, they deviate somewhat from the theoretical calculations. However, they exhibit an overall tendency consistent with the theoretical equations.

High-temperature thermal annealing has also been known to be effective in reducing other crystal defects, such as GBs and sub-grain boundaries (sub-GBs), as well as dislocations [96]. Further reduction was reported with increased annealing temperatures as the mobility of the crystal defects increases in the case of B-doped Si with a B impurity density less than 10^{19} cm^{-3} [123]. Furthermore, a reduction of sub-GBs, resulting from the annealing and elimination of the associated dislocations, was evident in the PL analysis.

4.2.3. *Effect of point defects*

A certain amount of energy, the so-called activation energy, has to be provided for the dislocations to overcome the barriers that they encounter during movement. Intrinsic point defects, such as vacancies and self-interstitials, as well as impurities, may have several significant effects on the magnitude of this activation energy. Some of these are beneficial, but most impede dislocation movement.

Studies using atomic-scale simulations have reported that, when a dislocation encounters vacancies or self-interstitial clusters in Si, it will pass through the clusters, and its slip velocity will decrease slightly, leading to up/down climbing of the dislocation. It will facilitate the annihilation of misfit dislocations owing to their opposite Burgers vectors, thereby reducing the threading dislocation density [124]. One study investigated the interaction between dislocations and two different types of vacancies subjected to an applied shear stress using a molecular dynamics simulation. The existence of V6-type vacancies was thought to decrease the slip velocity of the dislocation, as indicated by the work of Bolkhovityanov et al. [125]. On the other hand, the divacancy was found to have almost no influence on the slip velocity of the dislocation, which is consistent with the mechanism proposed by Kasper et al. [126]. The self-interstitial-cluster–dislocation interaction was studied via a molecular dynamics simulation at different temperatures and external loadings, and the I4 cluster was observed to be a barrier to dislocation motion by dragging the middle segment of the dislocation [127]. The concentration of vacancies and self-interstitials in Si is related to the ingot growth rate and growth temperature [117]. Vacancies remain in the crystal when the thermal gradient near the growth interface is small, while interstitial Si atoms generate Frank dislocation loops when the thermal gradient is large [128–131]. Hence, the equivalent recombination of vacancies with Si interstitial atoms provides defect-free crystals.

Stacking faults may also form strong barriers to lattice dislocation movement and to the formation of sub-grain boundaries. Stepped and curved stacking fault edges appear to generate dislocations. Their presence at elevated temperatures will therefore affect the overall dislocation mobility, including recovery processes, which has an impact on the evolution of the microstructure of residue dislocations and their density. Furthermore, stacking faults in mc-Si appear to be actively engaged in dislocation generation [132].

Oxygen, nitrogen, and hydrogen are most frequently found as non-metallic point defects in Si and these are known to significantly affect dislocation motion. The effect of shallow dopants on the dislocation behavior in Si was studied using a simple indentation technique [133], and non-electrically active dopants, such as nitrogen and oxygen, were reported to strongly impede dislocation motion. Contrary to oxygen and nitrogen, hydrogen was reported to lower the activation energy of dislocation movement; the formation energy for point defect decreases with the increase in the number of hydrogen atoms, so dislocation core states are passivated by hydrogen, thus reducing the activation energy for dislocation movement and enhancing dislocation velocity with rising hydrogen atom concentration [134].

A study using indentation tests at room temperature revealed that hydrogen is adsorbed on dislocations, diffuses along them, and changes electronic states. It was found that hydrogen also enhances dislocation mobility even at room temperature [135]. It was also reported that the velocity of dislocation motion was remarkably enhanced by the irradiation at temperatures below about 480 °C. The activation energy for dislocation glide was reduced to 1.2 eV under hydrogen plasma from 2.2 eV in the hydrogen-free condition [136]. Such hydrogen was thought to be trapped at some sites on the dislocation line and believed to interact with kinks, lowering the formation energy of these defects. At high temperatures, however, hydrogen rarely affects the dislocation annihilation at high temperatures. Fig. 6 shows the normalized intensity of FTIR spectroscopy peaks for hydrogen in mc-Si annealed up to 1100 °C in the present study. As shown, all the hydrogen diffused from Si before the dislocations were mobile enough to be annihilated.

Oxygen is an unavoidable impurity in Si, as it results from the dissolution of the walls of the silica crucible surrounding the melt. The first experimental observation of oxygen–dislocation interaction in 1975 concluded that neither interstitial oxygen nor SiO_2 precipitates had a pinning effect on dislocations [137]. Since then, however, reports using a variety of methods, such as indentation [138], in situ X-ray topographical techniques [139], and transmission electron microscopy [140], have shown that oxygen is effective at locking dislocations in Si. Furthermore, it was found to be possible for precipitates to form at the core of dislocations under particular annealing conditions, effectively impeding the dislocation motion. One study reported that oxygen precipitates with a density of 10^8–10^{10} cm^{-3} do not affect dislocation motion [141]. Conversely, small oxygen precipitates with a density on the order of 10^9 cm^{-3} exhibited a remarkable pinning effect on dislocation motion [137]. Hence, it is assumed that the pinning effect of oxygen precipitates on the dislocation motion is dependent on both their size and density [142]. Another study on dislocation locking by oxygen in Cz-Si showed that oxygen is capable of immobilizing dislocations in the 350–850 °C temperature range [143]. The shape of oxygen precipitates is also an important factor. Dislocation locking mainly involves a stress field interaction between precipitates and dislocations, and it was found that the interaction between dislocations and oxygen precipitates is more valid for platelet oxygen precipitates and likely less valid for polyhedral oxygen precipitates [144].

Since the late 1990s, there has been a drive to improve Si substrates with the deliberate addition of nitrogen to encourage oxygen precipitation for the collection of unwanted fast-diffusing metallic contaminants, in a process known as intrinsic gettering. Perhaps the simplest nitrogen defect in Si is substitutional nitrogen, lying on sites along [111]. However, the majority of nitrogen in Si takes the form of a dimer, N_2. The first research on the influence of nitrogen on the dislocation motion of Si was conducted by Sumino et al. in 1983 [145], and nitrogen was found to significantly immobilize the dislocations. Many other studies found that nitrogen interacts with dislocations and, moreover, can suppress interstitials and vacancy-related defects, thus introducing N-O complexes at high temperatures [146,147]. At lower temperatures, the reversed reaction becomes stable, and N_2V complexes can form again, thus suppressing vacancy aggregation. Recently, Giannattasio et al. [148] confirmed that nitrogen is highly effective at locking dislocations in FZ-Si and that the locking effect is similar to that of oxygen in Cz-Si. Sumino et al. [141] found, by means of tensile tests at high temperatures, that dislocations in nitrogen-doped Cz-Si are much slower than those in common Cz-Si, because the ejection of nitrogen impurities enhances the formation of small N-O complexes [149]. However, nitrogen's dislocation locking ability was found to fall to zero (within experimental error) at annealing temperatures above 1000 °C [150].

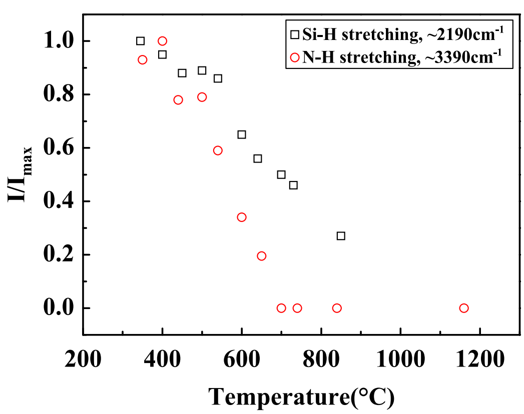

Fig. 6. Fourier Transform Infrared (FTIR) spectroscopy shows that hydrogen has diffused out of the samples by the time they reach roughly 1100 °C and before dislocation density reduction is observed. The above plot shows the normalized intensity of FTIR peaks involving hydrogen bonds.

To examine the effect of oxygen and nitrogen on dislocation density reduction, SiO_x and SiN_x were deposited on a 180-μm-thick mc-Si wafer, and the evolution of the dislocation density of the deposit and bare samples was measured after annealing at 1200 °C for 6 h. Fig. 7 shows the FTIR (Fig. 7(a)) and XRD (Fig. 7(b)) results of SiN_x-coated, SiO_x-coated, and bare mc-Si wafers ((*as-grown reference samples*)) annealed at 1200 °C for 6 h. The N–O complexes and oxygen peaks are observed for the samples with SiN_x and SiO_x films, respectively. Furthermore, except for the peaks for Si, nitrides and oxides were not detected in the XRD analysis, confirming that nitrogen and oxygen are perfectly dissolved in Si rather than forming compounds.

Fig. 8(a) shows dislocation etch-pit images for the samples after annealing and the measured evolution of dislocation density (N/N_0, where N is the initial dislocation density and N_0 is that after annealing) is plotted in Fig. 8(b). Bare Si exhibits ~12% dislocation density reduction, which is comparable with the results in Fig. 5. Interestingly, nitrogen is found to stimulate dislocation density reduction while oxygen locks dislocations, helps dislocation multiplication, and finally increases dislocation density. Although nitrogen is much more effective at locking than oxygen, the nitride film creates vacancies at the same time, stimulating the dislocation annihilation process [151].

According to the theory to account for the effect of doping on dislocation velocity, doping of dislocations with donors raises the Fermi level by increasing the electron concentration around the dislocations, which stimulates the formation of kinks and increases dislocation velocity. Conversely, doping with acceptors lowers the Fermi level and reduces the formation of kinks, thereby decreasing dislocation velocity. Indeed, an experimental study has shown that the velocity of dislocations at 800 °C in arsenic-doped Si is twice that in undoped Si [152]. Another measurement for boron-doped material revealed a fundamentally different behavior in the lower yield stress in comparison to phosphorus doping.

Transition metal impurities in Si are also of interest. The accumulation of impurity atoms at a dislocation core during annealing at high temperature may immobilize the dislocation. To move a locked dislocation, additional energy must be applied. The magnitude of this stress depends on the number of and nature (e.g., atoms, precipitates) of the impurities segregated to the dislocation core [153]. Nickel and copper metal impurities are primarily found at dislocations in as-grown crystals, and the release of these impurities from defects occurs rapidly. The gettering process is known to be effective at dissolving metal impurity precipitates to

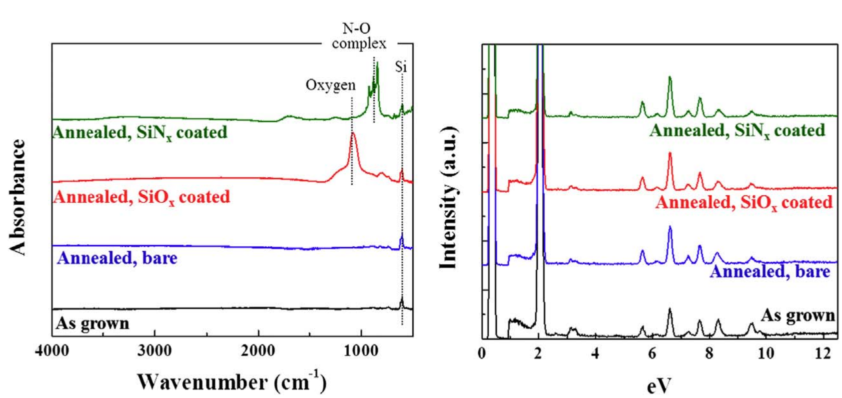

Fig. 7. (a) Fourier Transform Infrared (FTIR) spectroscopy; (b) X-ray diffraction (XRD) of SiNx coated, SiOx coated, bare mc-Si wafers, annealed at 1200 °C for 6 h, and an as-grown reference sample.

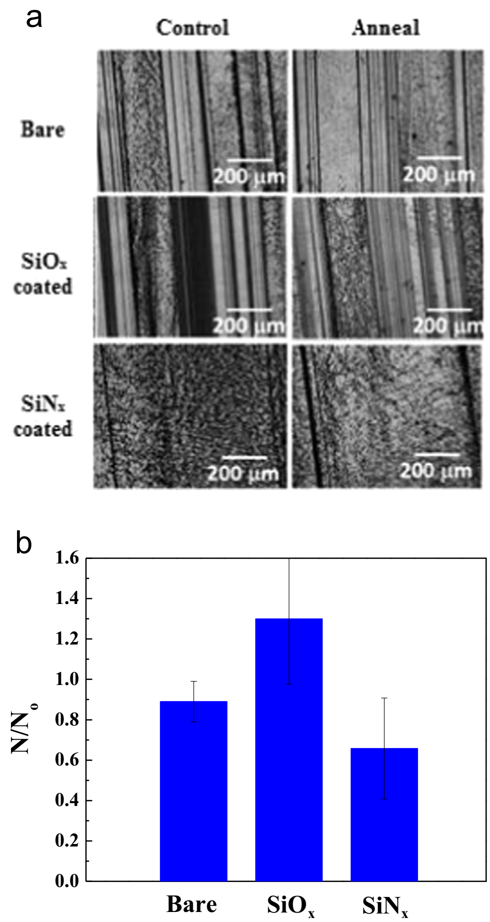

Fig. 8. (a) Dislocation etch-pit images; (b) dislocation density evolution for SiNx coated, SiOx coated, and bare mc-Si wafers annealed at 1200 °C for 6 h.

< 2–5 nm in size; however, the material performance was sometimes not greatly enhanced [153]. Under specific conditions, impurities play a positive role in removing dislocations [154]. An effort was made to annihilate dislocations in mc-Si at temperatures as low as 820 °C with the assistance of an additional driving force to stimulate dislocation motion. A reduction in dislocation density greater than 60% was observed for mc-Si with iron, copper, and nickel impurities in tens of parts per billion after phosphorus gettering at 820 °C. The hypothesis, supported by two different experiments, is that the net unidirectional flux of impurities in the presence of a gettering layer can cause dislocations to glide in a preferential direction and subsequently to sink at grain boundaries or surfaces. The minority carrier lifetime increases after phosphorus gettering, possibly as a result of the combined effects of dislocation density reduction and impurity concentration reduction.

4.2.4. *Effect of external stress*

Shear stress may enable dislocations to become mobile within certain crystallographic glide planes at temperatures above the brittle-to-ductile transition temperature (i.e., 530–660 °C for Si, depending on dopant concentration and strain rate) [114]. Furthermore, tensile or compressive stresses may promote mass flux, including vacancy diffusion, which helps dislocations to climb out of the glide plane at temperatures above 1000 °C. Hence, a sufficient amount of stresses may lead to enhancement of dislocation.

Bertoni et al. [116] reported that, after thermal annealing at 1350 °C and applying three-point bending, areas with > 10 MPa exhibited higher dislocation densities while areas with < 5 MPa were dislocation-free. Areas with tensile stress showed higher dislocation densities than those with equivalent compressive stress. The density appears to be sensitive to normal stress rather than shear. From this evidence, it is considered that atomic diffusion strongly involves the creep deformation in Si under certain conditions (i.e., < 5 MPa, 1350 °C). It might cause dislocations to be annealed out. Shear stress is a driving force for dislocation slip, whereas normal stress is a driving force for the diffusion of atoms or vacancies. Hence, the recovery might be sensitive to normal stress rather than shear stress. Furthermore, compression is a type of vacancy-closing mode, whereas tension is a vacancy-opening mode. Hence, atoms might diffuse to areas under compression and vacancies might diffuse to areas under tension, while dislocations under a small amount of compressive stress might be readily annealed out. An image force on the sample surface may help to annihilate more dislocations. Stokkan et al. [122] found a significant reduction in dislocation density near the sample surface (to a depth of ~50 μm from the surface), presumably due to the presence of an image force.

A pioneering experimental study by Samuels and Roberts clearly demonstrated a sharp transition from brittle-to-ductile behavior at a temperature above ~870 K [114]. However, dislocations can be generated at lower temperatures, even at room temperature, when the applied stress is sufficiently high [155]. Wu et al. [156,157] indicated that amorphization and dislocation nucleation are two dominant mechanisms and that the deformation sequence in nanoscratching is amorphization, stacking faults/twin development, and full dislocations. Some experimental results also indicated that dislocations can be mobile, even at temperatures below the brittle-to-ductile transition temperature.

The generation and emission of the first partial dislocation after phase transformation was observed under nanoscratching at room temperature [158]. It was revealed that impurity accumulation in Si can also be enhanced by the presence of stresses. This occurs at temperatures where both impurities and dislocations are mobile. The superposition of thermal stresses generates residual stress fields and dislocations, and, moreover, electrical activity increases at regions of higher dislocation densities and stresses [91].

From the perspective of electrical performance, low-stress or stress-free defect configurations are less likely to promote the gathering of metallic impurities at single dislocations or to generate new recombination-active dislocations under external mechanical and thermal stresses. Internal tensile or compressive stresses of several tens of megapascals are not thought to affect electrical activity through band structure modification but they can enhance the accumulation of metallic impurities and consequently the minority carrier recombination. High-magnetic-field treatment was found to have an apparent effect on dislocation–impurity interaction in Si [159]. Tension/compression load cycles at temperatures between 650 and 750 °C may induce resolved shear stresses on the primary slip system of 10–20 MPa. Both atomistic simulations and experiments showed that mobile dislocations strongly interact with point defects during their motion [72].

For other ceramic materials, such as undoped GaN, in-plane tensile stress, which is generated during film growth, can cause dislocations to become mobile and be released, producing arrays of a-type dislocations and reducing the overall dislocation density [160]. Interestingly, string ribbon mc-Si samples yielded an ~80% dislocation density reduction after annealing at 1200 °C in air for 6 h with the aid of compressive and tensile residual stress present during film growth, while only ~40% dislocations were annihilated under the same conditions when the residual stress was released by creating free surfaces.

5. Conclusions

This study reviewed the literature on the impact of dislocations on cell performance, the diagnosis of dislocations, and the engineering of dislocations during and after crystal growth, particularly focusing on multicrystalline silicon. The literature review on dislocations in multicrystalline silicon can be summarized as below.

(1) The impact of dislocations on the performance of Si solar cells: Dislocations, especially those decorated with impurities, have a negative impact on cell performance. In particular, interstitial iron and Fe-B pairs lead to a significant deterioration of the carrier lifetime. Furthermore, the influence of impurity-decorated dislocations on cell performance varies significantly with the distribution of these dislocations; photovoltaic efficiency is severely limited in hot spots (high-dislocation-density regions), owing to localized Joule heating.

(2) Diagnosis of dislocations in Si solar cells: To confirm the presence and determine the impact of dislocations, methods relying on photons or electrons (indirect observation techniques) have been used in combination with various microscopic techniques (direct observation techniques). Recent studies enable atomic-scale-resolution analysis of dislocations and impurities via TEM, AFM, and synchrotron X-ray-based techniques. At the same time, rapid dislocation diagnosis methods have been developed for in-line monitoring in industries.

(3) Dislocation engineering in Si solar cells: Significant effort has been expended in developing techniques that suppress the generation of dislocations during crystal growth or annihilate dislocations via post-annealing. The generation of dislocations can be suppressed by reducing the thermal stresses or by manipulating the crystal structures during crystal growth. Dislocation annihilation after crystal growth is affected primarily by the temperature, activation energy for dislocation movement, and stress. Although the dislocation density decreases with increasing annealing temperature and time, prolonged high-temperature annealing leads to significant contamination of the ingot and, consequently, deterioration of the minority carrier lifetime. The use of vacancies, foreign atoms (e.g., hydrogen, nitrogen or other impurities), and stresses has been attempted as means of providing additional energy that can replace the thermal energy. In particular, the unidirectional flux of impurities or a sufficient amount of stress may promote dislocation annihilation at temperatures below 1000 °C.

Acknowledgements

This research was supported by Leading Foreign Research Institute Recruitment Program through the National Research Foundation of Korea (NRF) funded by the Ministry of Science, ICT & Future Planning (MSIP) (2013K1A4A3055679). H. Choi also acknowledges the support of the NRF (NRF-2012-K1A3A1A30–054980). SC would like to thank the Roberto Rocca Fellowship Program.

References

[1] X. Gu, X. Yu, K. Guo, L. Chen, D. Wang, D. Yang, Seed-assisted cast quasi-single crystalline silicon for photovoltaic application: towards high efficiency and low cost silicon solar cells, Sol. Energy Mater. Sol. Cells 101 (2012) 95–101.
[2] D.M. Powell, M.T. Winkler, H.J. Choi, C.B. Simmons, D.B. Needleman, T. Buonassisi, Crystalline silicon photovoltaics: a cost analysis framework for determining technology pathways to reach baseload electricity costs, Energy Environ. Sci. 5 (2012) 5874–5883.
[3] P. Mints, J. Donnelly, Photovoltaic Manufacturing Shipments, Capacity & Competitive Analysis, Navigant Consulting, Inc., New York, 2012.
[4] B. Sopori, W. Chen, Influence of distributed defects on the photoelectric characteristics of a large-area device, J. Cryst. Growth 210 (2000) 375–378.
[5] A. Goetzberger, C. Hebling, Photovoltaic materials, past, present, future, Sol. Energy Mater. Sol. Cells 62 (2000) 1–19.
[6] US DOE, National PV Program "Five Year Research Plan", 1987.
[7] C. Donolato, Modeling the effect of dislocations on the minority carrier diffusion length of a semiconductor, J. Appl. Phys. 84 (1998) 2656–2664.
[8] S. Nakano, X.J. Chen, B. Gao, K. Kakimoto, Numerical analysis of cooling rate dependence on dislocation density in multicrystalline silicon for solar cells, J. Cryst. Growth 318 (2011) 280–282.
[9] J.C. Lambropoulos, C.H. Wu, Mechanics of shaped crystal growth from the melt, J. Mater. Res. 11 (1996) 2163–2176.
[10] Y. Nose, I. Takahashi, W. Pan, N. Usami, K. Fujiwara, K. Nakajima, Floating cast method to realize high-quality Si bulk multicrystals for solar cells, J. Cryst. Growth 311 (2009) 228–231.
[11] T.Y. Wang, S.L. Hsu, C.C. Fei, K.M. Yei, W.C. Hsu, C.W. Lan, Grain control using spot cooling in multi-crystalline silicon crystal growth, J. Cryst. Growth 311 (2009) 263–267.
[12] C. Reimann, T. Geiger, L. Sylla, J. Friedrich, Influencing the as grown dislocation density in directionally solidified multicrystalline silicon, in: Proceedings of the 7th International Workshop on Crystalline Silicon Solar Cells (CSSC7), Fukuoka, Japan, October 2013.
[13] G. Stokkan, E. Olsen, Influence of nucleation and contamination from crucible and coating on dislocation density and lifetime in multicrystalline silicon, in: Proceedings of the 22nd European Photovoltaic Solar Energy Conference and Exhibition, Milano, Italy, September 2007.
[14] H. Wang, H. Yang, H. Yu, G. Chen, Influence of gettering and passivation on uniformity of the electrical parameters in monolithic multicrystalline silicon solar cell, Solid State Phenom. 47 (2003) 1363–1367.
[15] S.A. McHugo, H. Hieslmair, E.R. Weber, Gettering of metallic impurities in photovoltaic silicon, Appl. Phys. A 64 (1997) 127–137.
[16] S.A. McHugo, W.D. Sawyer, Impurity decoration of defects in float zone and polycrystalline silicon via chemomechanical polishing, Appl. Phys. Lett. 62 (1993) 2519–2521.
[17] K. Arafune, T. Sasaki, F. Wakabayashi, Y. Terada, Y. Ohshita, M. Yamaguchi, Study on defects and impurities in cast-grown polycrystalline silicon substrates for solar cells, Physica B 376–377 (2006) 236–239.
[18] S. Mahajan, Defects in semiconductors and their effects on devices, Acta Mater. 48 (2000) 137–149.
[19] P. Omling, E. Weber, L. Montelius, H. Alexander, J. Michel, Electrical properties of dislocations and point defects in plastically deformed silicon, Phys. Rev. B 32 (1985) 6571.
[20] W.B. Jackson, N. Johnson, D. Biegelsen, Density of gap states of silicon grain boundaries determined by optical absorption, Appl. Phys. Lett. 43 (1983) 195–197.
[21] H.J. Möller, C. Funke, M. Rinio, S. Scholz, Multicrystalline silicon for solar cells, Thin Solid Films 487 (2005) 179–187.
[22] G. Wagner, H. Wawra, W. Dorsch, M. Albrecht, R. Krome, H.P. Strunk, S. Riedel, H.J. Möller, W. Appel, Structural and electrical properties of silicon epitaxial layers grown by LPE and CVD on identical polycrystalline substrates, J. Cryst. Growth 174 (1997) 680–685.
[23] H. El Ghitani, S. Martinuzzi, Modelling of the influence of dislocations on effective diffusion length and photocurrent of polycrystalline silicon cells, in: Proceedings of the 20th IEEE Photovoltaic Specialists Conference, (New York, USA), September 1988, pp. 1624–1628.
[24] T. Arguirov, T. McHedlidze, M. Kittler, M. Reiche, T. Wilhelm, T. Hoang, J. Holleman, J. Schmitz, Silicon based light emitters utilizing radiation from dislocations; electric field induced shift of the dislocation-related luminescence, Physica E 41 (2009) 907–911.
[25] J. Haunschild, M. Glatthaar, M. Demant, J. Nievendick, M. Motzko, S. Rein, E. R. Weber, Quality control of as-cut multicrystalline silicon wafers using photoluminescence imaging for solar cell production, Sol. Energy Mater. Sol. Cells 94 (2010) 2007–2012.
[26] I. Tarasov, S. Ostapenko, W. Seifert, M. Kittler, J.P. Kaleis, Defect diagnostics in multicrystalline silicon using scanning techniques, Physica B 308–310 (2001) 1133–1136.
[27] S. Wu, L. Wang, X. Li, P. Wang, D. Yang, D. You, J. Du, T. Zhang, Y. Wan, Influence of defects and impurities on the deteriorated border region in multicrystalline silicon ingots, Cryst. Res. Technol. 47 (2012) 7–12.
[28]] U. Hess, P.Y. Pichon, S. Seren, A. Schönecker, G. Hahn, Crystal defects and their impact on ribbon growth on substrate (RGS) silicon solar cells, Sol. Energy Mater. Sol. Cells 117 (2013) 471–475.
[29] A. Eyer, I. Reis, Defects in crystalline silicon for solar cells (DIXSI): a co-operative German research project, in: Proceedings of the 24th IEEE Photovoltaic Specialists Conference, (Waikoloa, Hawaii), December 1994, pp. 1587–1590.
[30] A. Simo, S. Martinuzzi, Hot spots and heavily dislocated regions in multicrystalline silicon cells, in: Proceedings of the 21st IEEE Photovoltaic Specialists Conference, (Orlando, USA), May 1990, pp. 800–805.

[31] T. Arguirov, M. Kittler, W. Seifert, X. Yu, M. Reiche, Towards silicon based light emitter utilising the radiation from dislocation networks, Mater. Sci. Eng. B 134 (2006) 109–113.
[32] M. Lourenço, M. Milosavljević, G. Shao, R. Gwilliam, K. Homewood, Boron engineered dislocation loops for efficient room temperature silicon light emitting diodes, Thin solid films 504 (2006) 36–40.
[33] G. Jia, W. Seifert, T. McHedlidze, T. Arguirov, M. Kittler, T. Wilhelm, M. Reiche, EBIC/PL investigations of dislocation network produced by silicon wafer direct bonding, Superlattices Microstruct. 45 (2009) 314–320.
[34] W. Dash, Copper precipitation on dislocations in silicon, J. Appl. Phys. 27 (1956) 1193–1195.
[35] E. Sirtl, A. Adler, Chromic acid-hydrofluoric acid as specific reagents for the development of etching pits in silicon, Z. Met. ZEMTA 52 (1961) 529.
[36] M.W. Jenkins, A new preferential etch for defects in silicon crystals, J. Electrochem. Soc. 124 (1977) 757–762.
[37] F.S. d'Aragona, Dislocation etch for (100) planes in silicon, J. Electrochem. Soc. 119 (1972) 948–951.
[38] D. Schimmel, A comparison of chemical etches for revealing ⟨100⟩ silicon crystal defects, J. Electrochem. Soc. 123 (1976) 734–741.
[39] B. Sopori, A new defect etch for polycrystalline silicon, J. Electrochem. Soc. 131 (1984) 667–672.
[40] V. Schneider, C. Reimann, J. Friedrich, M. Müller, Reusable crucible for directional solidification of silicon: Impact of crucible purity, in: Proceedings of 7th International Workshop on Crystalline Silicon Solar Cells, Fukuoka, Japan, October 2013.
[41] H. Idrisi, T. Sinke, V. Gerhardt, D. Ceglarek, B.O. Kolbesen, Decoration and preferential etching of crystal defects in silicon materials: influence of metal decoration on the defect etching process, Phys. Status Solidi C 8 (2011) 788–791.
[42] J.D. Murphy, C.R. Alpass, A. Giannattasio, S. Senkader, R.J. Falster, P. R. Wilshaw, Nitrogen in silicon: transport and mechanical properties, Nucl. Instrum. Methods Phys. B 253 (2006) 113–117.
[43] D. Li, D. Yang, D. Que, Effects of nitrogen on dislocations in silicon during heat treatment, Physica B 273–274 (1999) 553–556.
[44] M.M.L. Vogl, Dislocation Density Reduction in Multicrystalline Silicon Through Cyclic Annealing S.M. thesis, Massachusetts Institute of Technology, 2011.
[45] D.B. Needleman, H. Choi, D.M. Powell, T. Buonassisi, Rapid dislocation-density mapping of as-cut crystalline silicon wafers, Phys. Status Solidi (RRL) 7 (2013) 1041–1044.
[46] G. Stokkan, Relationship between dislocation density and nucleation of multicrystalline silicon, Acta Mater. 58 (2010) 3223–3229.
[47] M.P. Bellmann, T. Kaden, D. Kressner-Kiel, J. Friedl, H.J. Möller, L. Arnberg, The impact of germanium doping on the dislocation distribution in directional solidified mc-silicon, J. Cryst. Growth 325 (2011) 1–4.
[48] E. Schmid, C. Funke, T. Behm, O. Pätzold, H. Berek, M. Stelter, Investigation of dislocation structures in ribbon- and ingot-grown multicrystalline silicon, J. Cryst. Growth 382 (2013) 41–46.
[49] M. Sato, K. Hiraga, K. Sumino, HVEM structure images of extended 60°-and screw dislocations in silicon, Jpn. J. Appl. Phys. 19 (1980) L155.
[50] H. Kolar, J. Spence, H. Alexander, Observation of moving dislocation kinks and unpinning, Phys. Rev. Lett. 77 (1996) 4031.
[51] J.B. Newkirk, Method for the detection of dislocations in silicon by X-ray extinction contrast, Phys. Rev. 110 (1958) 1465–1466.
[52] M. Lourenco, M. Milosavljević, G. Shao, R. Gwilliam, K. Homewood, Dislocation engineered silicon light emitting devices, Thin Solid Films 515 (2007) 8113–8117.
[53] F. Cristiano, B. Colombeau, J. Grisolia, B. de Mauduit, F. Giles, M. Omri, D. Skarlatos, D. Tsoukalas, A. Claverie, Influence of the annealing ambient on the relative thermal stability of dislocation loops in silicon, Nucl. Instrum. Methods Phys. B 178 (2001) 84–88.
[54] M. Legros, A. Jacques, A. George, Cyclic deformation of silicon single crystals: mechanical behaviour and dislocation arrangements, Mater. Sci. Eng. A 387–389 (2004) 495–500.
[55] K. Higashida, T. Kawamura, T. Morikawa, Y. Miura, N. Narita, R. Onodera, HVEM observation of crack tip dislocations in silicon crystals, Mater. Sci. Eng. A 319–321 (2001) 683–686.
[56] J. Rabier, M.F. Denanot, J.L. Demenet, P. Cordier, Plastic deformation by shuffle dislocations in silicon, Mater. Sci. Eng. A 387–389 (2004) 124–128.
[57] N. Osakabe, K. Yagi, G. Honjo, Reflection electron microscope observations of dislocations and surface structure phase transition on clean (111) silicon surfaces, Jpn. J. Appl. Phys. 19 (1980) L309.
[58] M. Tanaka, K. Higashida, K. Kaneko, S. Hata, M. Mitsuhara, Crack tip dislocations revealed by electron tomography in silicon single crystal, Scr. Mater. 59 (2008) 901–904.
[59] S. Pan, I.V. Mitchell, Effect of interaction between point defects and pre-existing dislocation loops on anomalous B diffusion in silicon, Mater. Chem. Phys. 46 (1996) 252–258.
[60] C.J. Fall, J.P.G. Goss, R. Jones, P.R. Briddon, A.T. Blumenau, T. Frauenheim, Modelling electron energy-loss spectra of dislocations in silicon and diamond, Physica B 308–310 (2001) 577–580.
[61] K. Hoummada, D. Mangelinck, B. Gault, M. Cabié, Nickel segregation on dislocation loops in implanted silicon, Scr. Mater. 64 (2011) 378–381.
[62] A. Portavoce, G. Tréglia, Theoretical investigation of Cottrell atmosphere in silicon, Acta Mater. 65 (2014) 1–9.
[63] G. Golan, E. Rabinovich, A. Inberg, A. Axelevitch, M. Oksman, Y. Rosenwaks, A. Kozlovsky, P.G. Rancoita, M. Rattaggi, A. Seidman, N. Croitoru, Dislocations structure investigation in neutron irradiated silicon detectors using AFM and microhardness measurements, Microelectron. Reliab. 39 (1999) 1497–1504.
[64] T. Chu, M. Yamada, J. Donecker, M. Rossberg, V. Alex, H. Riemann, Optical anisotropy and strain-induced birefringence in dislocation-free silicon single crystals, Mater. Sci. Eng. B 91–92 (2002) 174–177.
[65] D. Lowney, T. Perova, M. Nolan, P. McNally, R. Moore, H. Gamble, T. Tuomi, R. Rantamäki, A. Danilewsky, Investigation of strain induced effects in silicon wafers due to proximity rapid thermal processing using micro-Raman spectroscopy and synchrotron x-ray topography, Semicond. Sci. Technol. 17 (2002) 1081.
[66] A.N. Danilewsky, A. Rack, J. Wittge, T. Weitkamp, R. Simon, H. Riesemeier, T. Baumbach, White beam synchrotron topography using a high resolution digital X-ray imaging detector, Nucl. Instrum. Methods Phys. B 266 (2008) 2035–2040.
[67] A.N. Danilewsky, R. Simon, A. Fauler, M. Fiederle, K.W. Benz, White beam X-ray topography at the synchrotron light source ANKA, Research Centre Karlsruhe, Nucl. Instrum. Methods Phys. B 199 (2003) 71–74.
[68] D. Allen, J. Wittge, A. Zlotos, E. Gorostegui-Colinas, J. Garagorri, P.J. McNally, A.N. Danilewsky, M.R. Elizalde, Observation of nano-indent induced strain fields and dislocation generation in silicon wafers using micro-Raman spectroscopy and white beam X-ray topography, Nucl. Instrum. Methods Phys. B 268 (2010) 383–387.
[69] D. Oriwol, E.R. Carl, A.N. Danilewsky, L. Sylla, W. Seifert, M. Kittler, H. S. Leipner, Small-angle subgrain boundaries emanating from dislocation pile-ups in multicrystalline silicon studied with synchrotron white-beam X-ray topography, Acta Mater. 61 (2013) 6903–6910.
[70] J. Parsons, C.S. Beer, D.R. Leadley, A.D. Capewell, T.J. Grasby, Evaluation of relaxation and misfit dislocation blocking in strained silicon on virtual substrates, Thin Solid Films 517 (2008) 17–19.
[71] A.N. Danilewsky, J. Wittge, A. Croell, D. Allen, P. McNally, P. Vagovič, T. dos Santos Rolo, Z. Li, T. Baumbach, E. Gorostegui-Colinas, J. Garagorri, M. R. Elizalde, M.C. Fossati, D.K. Bowen, B.K. Tanner, Dislocation dynamics and slip band formation in silicon: in-situ study by X-ray diffraction imaging, J. Cryst. Growth 318 (2011) 1157–1163.
[72] J.P. Feiereisen, O. Ferry, A. Jacques, A. George, Mechanical testing device for in situ experiments on reversibility of dislocation motion in silicon, Nucl. Instrum. Methods Phys. B 200 (2003) 339–345.
[73] Y. Wang, K. Kakimoto, An in-situ X-ray topography observation of dislocations, crystal–melt interface and melting of silicon, Microelectron. Eng. 56 (2001) 143–146.
[74] J.J. Simon, I. Périchaud, Influence of oxygen on the recombination strength of dislocations in silicon wafers, Mater. Sci. Eng. B 36 (1996) 183–186.
[75] F. Vallino, J.-P. Château, A. Jacques, A. George, Dislocation multiplication during the very first stages of plastic deformation in silicon observed by X-ray topography, Mater. Sci. Eng. A 319–321 (2001) 152–155.
[76] J. Yi, Y. Chu, T. Argunova, J. Je, Analytic determination of the three-dimensional distribution of dislocations using synchrotron X-ray topography, J. Appl. Cryst. 39 (2006) 106–108.
[77] M.G. Tsoutsouva, V.A. Oliveira, D. Camel, T.N. Tran Thi, J. Baruchel, B. Marie, T. A. Lafford, Segregation, precipitation and dislocation generation between seeds in directionally solidified mono-like silicon for photovoltaic applications, J. Cryst. Growth 401 (2014) 397–403.
[78] B. Shen, T. Sekiguchi, R. Zhang, Y. Shi, H. Shi, K. Yang, Y. Zheng, K. Sumino, Precipitation of Cu and Fe in dislocated floating-zone-grown silicon, Jpn. J. Appl. Phys. 35 (1996) 3301.
[79] I. Tarasov, S. Ostapenko, C. Haessler, E.U. Reisner, Spatially resolved defect diagnostics in multicrystalline silicon for solar cells, Mater. Sci. Eng. B 71 (2000) 51–55.
[80] I. Capan, V. Borjanović, B. Pivac, Dislocation-related deep levels in carbon rich p-type polycrystalline silicon, Sol. Energy Mater. Sol. Cells 91 (2007) 931–937.
[81] N. Yarykin, E. Steinman, Comparative study of the plastic deformation- and implantation-induced centers in silicon, Physica B 340–342 (2003) 756–759.
[82] B. Pichaud, G. Mariani-Regula, E.B. Yakimov, Interaction of gold with dislocations in silicon, Mater. Sci. Eng. B 71 (2000) 272–275.
[83] M. Ogawa, S. Kamiya, H. Izumi, Y. Tokuda, Electronic properties of dislocations introduced mechanically at room temperature on a single crystal silicon surface, Physica B 407 (2012) 3034–3037.
[84] I. Périchaud, J.J. Simon, S. Martinuzzi, LBIC investigation of impurity-dislocation interaction in FZ silicon wafers, Mater. Sci. Eng. B 42 (1996) 265–269.
[85] R. Slunjski, I. Capan, B. Pivac, A. Le Donne, S. Binetti, Effects of low-temperature annealing on polycrystalline silicon for solar cells, Sol. Energy Mater. Sol. Cells 95 (2011) 559–563.
[86] C. Modanese, L. Arnberg, M. Di Sabatino, Analysis of impurities with inhomogeneous distribution in multicrystalline solar cell silicon by glow discharge mass spectrometry, Mater. Sci. Eng. B 180 (2014) 27–32.
[87] S. Rein, S.W. Glunz, Electronic properties of interstitial iron and iron-boron pairs determined by means of advanced lifetime spectroscopy, J. Appl. Phys. 98 (2005) 113711.
[88] J.E. Birkholz, K. Bothe, D. Macdonald, J. Schmidt, Electronic properties of iron-boron pairs in crystalline silicon by temperature- and injection-level-dependent lifetime measurements, J. Appl. Phys. 97 (2005) 103708.

[89] R. Zierer, T. Kaden, S. Würzner, H.J. Möller, The Distribution of interstitial iron at dislocation clusters at elevated temperature, Energy Procedia 38 (2013) 649–657.
[90] M. Fukuzawa, M. Yamada, Photoelastic characterization of Si wafers by scanning infrared polariscope, J. Cryst. Growth 229 (2001) 22–25.
[91] G. Sarau, S. Christiansen, M. Holla, W. Seifert, Correlating internal stresses, electrical activity and defect structure on the micrometer scale in EFG silicon ribbons, Sol. Energy Mater. Sol. Cells 95 (2011) 2264–2271.
[92] J. Spence, C. Koch, Experimental evidence for dislocation core structures in silicon, Scr. Mater. 45 (2001) 1273–1278.
[93] L. Gong, F. Wang, Q. Cai, D. You, B. Dai, Characterization of defects in mono-like silicon wafers and their effects on solar cell efficiency, Sol. Energy Mater. Sol. Cells 120 (2014) 289–294.
[94] H. Sugimoto, K. Araki, M. Tajima, T. Eguchi, I. Yamaga, M. Dhamrin, K. Kamisako, T. Saitoh, Photoluminescence analysis of intragrain defects in multicrystalline silicon wafers for solar cells, J. Appl. Phys. 102 (2007) 054506.
[95] D.J. Stowe, S.A. Galloway, S. Senkader, K. Mallik, R.J. Falster, P.R. Wilshaw, Near-band gap luminescence at room temperature from dislocations in silicon, Physica B 340–342 (2003) 710–713.
[96] H. Kim, J. Lee, C. Lee, J. Kim, B.-y. Jang, J. Lee, W. Yoon, Effect of heat treatment of spin-cast solar silicon sheet on crystalline defects, Curr. Appl. Phys. 13 (Supplement 2) (2013) S88–S92.
[97] T.U. Nærland, L. Arnberg, A. Holt, Origin of the low carrier lifetime edge zone in multicrystalline PV silicon, Prog. Photovolt.: Res. Appl. 17 (2009) 289–296.
[98] D. You, J. Du, T. Zhang, Y. Wan, W. Shan, L. Wang, D. Yang, The dislocation distribution characteristics of a multi-crystalline silicon ingot and its impact on the cell efficiency, in: Proceedings of the 35th IEEE Photovoltaic Specialists Conference, (Honolulu, USA), June 2010, pp. 2258–2261.
[99] B. Ryningen, G. Stokkan, M. Kivambe, T. Ervik, O. Lohne, Growth of dislocation clusters during directional solidification of multicrystalline silicon ingots, Acta Mater. 59 (2011) 7703–7710.
[100] D. Franke, T. Rettelbach, C. Häßler, W. Koch, A. Müller, Silicon ingot casting: process development by numerical simulations, Sol. Energy Mater. Sol. Cells 72 (2002) 83–92.
[101] H.-j. Su, J. Zhang, L. Liu, H.-z. Fu, Preparation, microstructure and dislocation of solar-grade multicrystalline silicon by directional solidification from metallurgical-grade silicon, Trans. Nonferrous Met. Soc. China 22 (2012) 2548–2553.
[102] N. Chen, S. Qiu, B. Liu, G. Du, G. Liu, W. Sun, An optical microscopy study of dislocations in multicrystalline silicon grown by directional solidification method, Mater. Sci. Semicond. Process. 13 (2010) 276–280.
[103] D. Oriwol, M. Hollatz, M. Reinecke, Control of dislocation cluster formation and development in silicon block casting, Energy Procedia 27 (2012) 66–69.
[104] B. Gao, K. Kakimoto, Numerical investigation of the influence of cooling flux on the generation of dislocations in cylindrical mono-like silicon growth, J. Cryst. Growth 384 (2013) 13–20.
[105] K. Fujiwara, K. Maeda, N. Usami, G. Sazaki, Y. Nose, K. Nakajima, Formation mechanism of parallel twins related to Si-facetted dendrite growth, Scr. Mater. 57 (2007) 81–84.
[106] K. Fujiwara, K. Maeda, N. Usami, K. Nakajima, Growth mechanism of Si-faceted dendrites, Phys. Rev. Lett. 101 (2008) 055503.
[107] K. Fujiwara, K. Maeda, N. Usami, G. Sazaki, Y. Nose, A. Nomura, T. Shishido, K. Nakajima, In situ observation of Si faceted dendrite growth from low-degree-of-undercooling melts, Acta Mater. 56 (2008) 2663–2668.
[108] J.P. Hirth, J. Lothe, Theory of Dislocations, Wiley, New York, 1982.
[109] A. Gulluoglu, C. Hartley, Simulation of dislocation microstructures in two dimensions. II. Dynamic and relaxed structures, Model. Simul. Mater. Sci. Eng. 1 (1993) 383.
[110] D.L. Olmsted, L.G. Hector Jr, W. Curtin, R. Clifton, Atomistic simulations of dislocation mobility in Al, Ni and Al/Mg alloys, Model. Simul. Mater. Sci. Eng. 13 (2005) 371.
[111] M. Li, W. Chu, K. Gao, L. Qiao, Molecular dynamics simulation of cross-slip and the intersection of dislocations in copper, J. Phys. 15 (2003) 3391.
[112] C.-x. Li, Q.-y. Meng, G. Li, L.-j. Yang, Atomistic simulation of the 60° dislocation mobility in silicon crystal, Superlattices Microstruct. 40 (2006) 113–118.
[113] J. Eshelby, Supersonic dislocations and dislocations in dispersive media, Proc. Phys. Soc. Sect. B 69 (1956) 1013.
[114] J. Samuels, S. Roberts, The brittle-ductile transition in silicon I. Experiments, Proc. R. Soc. Lond. A 421 (1989) 1–23.
[115] K. Hartman, M. Bertoni, J. Serdy, T. Buonassisi, Dislocation density reduction in multicrystalline silicon solar cell material by high temperature annealing, Appl. Phys. Lett. 93 (2008) 122108-122108-3.
[116] M.I. Bertoni, C. Colin, T. Buonassisi, Dislocation engineering in multicrystalline silicon, Solid State Phenom. 156 (2010) 11–18.
[117] T. Abe, T. Takahashi, Intrinsic point defect behavior in silicon crystals during growth from the melt: a model derived from experimental results, J. Cryst. Growth 334 (2011) 16–36.
[118] D. Kuhlmann, On the theory of plastic deformation, Proc. Phys. Soc. A 64 (1951) 140.
[119] E. Nes, Recovery revisited, Acta Metall. Mater. 43 (1995) 2189–2207.
[120] H. Xu, R. Hong, H. Shen, Effects of high temperature annealing on the dislocation density and electrical properties of upgraded metallurgical grade multicrystalline silicon, Chin. Sci. Bull. 56 (2011) 695–699.
[121] H.-j. Wu, W.-h. Ma, X.-h. Chen, Y. Jiang, X.-y. Mei, C. Zhang, X.-h. Wu, Effect of thermal annealing on defects of upgraded metallurgical grade silicon, Trans. Nonferrous Met. Soc. China 21 (2011) 1340–1347.
[122] G. Stokkan, C. Rosario, M. Berg, O. Lohne, High temperature annealing of dislocations in multicrystalline silicon for solar cells, Sol. Power (2012).
[123] T. Makino, H. Nakamura, Resistivity changes of heavily-boron-doped CVD-prepared polycrystalline silicon caused by thermal annealing, Solid State Phenom. 24 (1981) 49–55.
[124] C. Li, Q. Meng, Computer simulation of the vacancy defects interaction with shuffle dislocation in silicon, Superlattices Microstruct. 45 (2009) 1–7.
[125] Y.B. Bolkhovityanov, A.S. Deryabin, A.K. Gutakovskii, M.A. Revenko, L. V. Sokolov, Heterostructures $GexSi1-x/Si(001)$ $(x=0.18–0.62)$ grown by molecular beam epitaxy at a low (350 °C) temperature: specific features of plastic relaxation, Thin Solid Films 466 (2004) 69–74.
[126] E. Kasper, K. Lyutovich, M. Bauer, M. Oehme, New virtual substrate concept for vertical MOS transistors, Thin Solid Films 336 (1998) 319–322.
[127] Y. Jing, Q. Meng, W. Zhao, Molecular dynamics simulations of the interaction between 60° dislocation and self-interstitial cluster in silicon, Physica B 404 (2009) 2138–2141.
[128] P.J. Roksnoer, M.M.B. van den Boom, Microdefects in a non-striated distribution in floating-zone silicon crystals, J. Cryst. Growth 53 (1981) 563–573.
[129] J. Ryuta, E. Morita, T. Tanaka, Y. Shimanuki, Crystal-originated singularities on Si wafer surface after SC1 cleaning, Jpn. J. Appl. Phys. 29 (1990) L1947.
[130] M. Itsumi, H. Akiya, T. Ueki, M. Tomita, M. Yamawaki, The composition of octahedron structures that act as an origin of defects in thermal SiO2 on Czochralski silicon, J. Appl. Phys. 78 (1995) 5984–5988.
[131] H. Föll, B.O. Kolbesen, Formation and nature of swirl defects in silicon, Appl. Phys. 8 (1975) 319–331.
[132] M.M. Kivambe, T. Ervik, B. Ryningen, G. Stokkan, On the role of stacking faults on dislocation generation and dislocation cluster formation in multicrystalline silicon, J. Appl. Phys. 112 (2012) 103528.
[133] S. Roberts, P. Pirouz, P. Hirsch, A simple technique for measuring doping effects on dislocation motion in silicon, J. Phys. Colloq. 44 (1983), C4–75-C74-C83.
[134] N. Martsinovich, A.L. Rosa, M.I. Heggie, C.P. Ewels, P.R. Briddon, Density-functional theory calculations on H defects in Si, Physica B 340–342 (2003) 654–658.
[135] M. Ogawa, S. Kamiya, H. Izumi, Y. Tokuda, Effect of hydrogen at room temperature on electronic and mechanical properties of dislocations in silicon, Mater. Lett. 120 (2014) 236–238.
[136] Y.Y. Yamashita, F. Jyobe, Y. Kamiura, K. Maeda, Effects of hydrogen plasma on dislocation motion in silicon, Mater. Sci. Forum 258 (1997) 313–318.
[137] S. Hu, W. Patrick, Effect of oxygen on dislocation movement in silicon, J. Appl. Phys. 46 (1975) 1869–1874.
[138] S. Hu, A method for finding critical stresses of dislocation movement, Appl. Phys. Lett. 31 (1977) 139–141.
[139] K. Sumino, H. Harada, In situ X-ray topographic studies of the generation and the multiplication processes of dislocations in silicon crystals at elevated temperatures, Philos. Mag. A 44 (1981) 1319–1334.
[140] S. Senkader, K. Jurkschat, P.R. Wilshaw, R.J. Falster, A study of oxygen dislocation interactions in CZ-Si, Mater. Sci. Eng. B 73 (2000) 111–115.
[141] I. Yonenaga, K. Sumino, K. Hoshi, Mechanical strength of silicon crystals as a function of the oxygen concentration, J. Appl. Phys. 56 (1984) 2346–2350.
[142] Z. Zeng, X. Ma, J. Chen, D. Yang, I. Ratschinski, F. Hevroth, H.S. Leipner, Effect of oxygen precipitates on dislocation motion in Czochralski silicon, J. Cryst. Growth 312 (2010) 169–173.
[143] J.D. Murphy, S. Senkader, R.J. Falster, P.R. Wilshaw, Oxygen transport in Czochralski silicon investigated by dislocation locking experiments, Mater. Sci. Eng. B 134 (2006) 176–184.
[144] Z. Zeng, J. Chen, Y. Zeng, X. Ma, D. Yang, Immobilization of dislocations by oxygen precipitates in Czochralski silicon: Feasibility of precipitation strengthening mechanism, J. Cryst. Growth 324 (2011) 93–97.
[145] K. Sumino, I. Yonenaga, M. Imai, T. Abe, Effects of nitrogen on dislocation behavior and mechanical strength in silicon crystals, J. Appl. Phys. 54 (1983) 5016–5020.
[146] T. Abe, H. Takeno, Dynamic behavior of intrinsic point defects in FZ and CZ silicon crystals, in: Proceedings of the Materials Research Society, San Francisco, USA, April 1992.
[147] W.V. Ammon, P. Dreier, W. Hensel, U. Lambert, L. Köster, Influence of oxygen and nitrogen on point defect aggregation in silicon single crystals, Mater. Sci. Eng. B 36 (1996) 33–41.
[148] A. Giannattasio, S. Senkader, R.J. Falster, P.R. Wilshaw, Dislocation locking by nitrogen impurities in FZ-silicon, Physica B 340–342 (2003) 996–1000.
[149] L. Jastrzebski, G. Cullen, R. Soydan, G. Harbeke, J. Lagowski, S. Vecrumba, W. Henry, The effect of nitrogen on the mechanical properties of float zone silicon and on CCD device performance, J. Electrochem. Soc. 134 (1987) 466–470.
[150] C. Alpass, J.D. Murphy, R. Falster, P. Wilshaw, Nitrogen diffusion and interaction with dislocations in single-crystal silicon, J. Appl. Phys. 105 (2009) 013519.
[151] A. Giannattasio, S. Senkader, R. Falster, P. Wilshaw, Dislocation locking by nitrogen impurities in FZ-silicon, Physica B 340 (2003) 996–1000.
[152] J. Patel, P. Freeland, Change of dislocation velocity with Fermi level in silicon, Phys. Rev. Lett. 18 (1967) 833.
[153] S.A. McHugo, Release of metal impurities from structural defects in polycrystalline silicon, Appl. Phys. Lett. 71 (1997) 1984–1986.

[154] H. Choi, M. Bertoni, J. Hofstetter, D. Fenning, D. Powell, S. Castellanos, T. Buonassisi, Dislocation density reduction during impurity gettering in multicrystalline silicon, Photovolt. IEEE J. 3 (2013) 189–198.
[155] C. Thaulow, D. Sen, M.J. Buehler, Atomistic study of the effect of crack tip ledges on the nucleation of dislocations in silicon single crystals at elevated temperature, Mater. Sci. Eng. A 528 (2011) 4357–4364.
[156] Y. Wu, H. Huang, J. Zou, L. Zhang, J. Dell, Nanoscratch-induced phase transformation of monocrystalline Si, Scr. Mater. 63 (2010) 847–850.
[157] Y.Q. Wu, H. Huang, J. Zou, J.M. Dell, Nanoscratch-induced deformation of single crystal silicon, J. Vac. Sci. Technol. B 27 (2009) 1374–1377.
[158] Q.H. Fang, L.C. Zhang, Prediction of the threshold load of dislocation emission in silicon during nanoscratching, Acta Mater. 61 (2013) 5469–5476.
[159] I. Yonenaga, K. Takahashi, T. Taishi, Y. Ohno, Influence of high-magnetic-field on dislocation–oxygen interaction in silicon, Physica B 401–402 (2007) 148–150.
[160] M. Moram, M. Kappers, F. Massabuau, R. Oliver, C. Humphreys, The effects of Si doping on dislocation movement and tensile stress in GaN films, J. Appl. Phys. 109 (2011) 073509.